NAIC-ID(RS)T-0536-96

NATIONAL AIR INTELLIGENCE CENTER

SELECTED ARTICLES

Approved for public release: distribution unlimited

HUMAN TRANSLATION

NAIC-ID(RS)T-0536-96 21 January 1997

MICROFICHE NR:

SELECTED ARTICLES

English pages: 45

Source: Unknown

Country of origin: China
Translated by: Leo Kanner Associates
F33657-88-D-2188
Requester: NAIC/TAEC/Frank Scenna
Approved for public release: distribution unlimited.

PREPARED BY:

TRANSLATION SERVICES
NATIONAL AIR INTELLIGENCE CENTER
WPAFB, OHIO

TABLE OF CONTENTS

GRAPHICS DISCLAIMER

All figures, graphics, tables, equations, etc. merged into this translation were extracted from the best quality copy available.

ANALYSIS OF FREQUENCY SPECTRUM OF COHERENT PULSE DOPPLER RADAR DURING VELOCITY INTERFERENCE*

Wang Wantong

Research Institute No. 29
Ministry of Electronic Industry, Chengdu

ABSTRACT: This paper describes the feasibility of convolution integration and waveform integration methods in analyzing the frequency spectrum properties of pulse Doppler (PD) radars, and realizing frequency agility. It is concluded that phase modulation frequency shifting, which was designed for jamming continuous wave (CW) radars, is also available for jamming coherent PD radars.

KEY WORDS: pulse signal modulation, pulse Doppler radar, frequency spectrum, velocity jamming, frequency shifting.

0. Introduction

It is well known that CW wave radars and pulse Doppler (PD) radars can be used to measure velocity, based on the unique relationship between Doppler frequency and relative target velocity. By modifying the frequency of a radar signal (radar

* This paper was accredited as an outstanding paper presented at 95 Annual Academic Conference sponsored by Research Institute No. 29, Ministry of Electronics.

return), phase modulation frequency shifting can realize velocity jamming of CW radars with respect to continuous waves. Likewise, this paper analyzed the feasibility of applying this principle in realizing velocity jamming of PD radars through frequency shifting.

1. Realization of Sawtooth Wave Modulation Within Pulse Width

When signals are input by continuous waves, sawtooth waves as signal-modulating waves can be used at any time to modulate the signals, and the modulation result will stay unchanged as long as the optimal modulation conditions can be met. Now, we use the same sawtooth waves to modulate pulse signals. Since radio frequency signals are discontinuous in pulse intervals, the modulation of sawtooth waves that are broader than the pulse width will also be discontinuous.

Since the pulse width is fairly narrow, the period of sawtooth waves used to modulate within the pulse width will be correspondingly smaller, and the frequency shift value correspondingly will be larger and may even overreach the passband of a set of velocity filters, thus failing to attain the optimal jamming effect. Under such circumstances, the analysis given in this section must be limited to the modulation of optimal sawtooth waves within the maximum pulse width.

First of all, we must demonstrate that by using a single sawtooth wave to modulate within a single pulse width, the optimal frequency shift can also be realized as confirmed by the waveforms shown in Fig. 1.

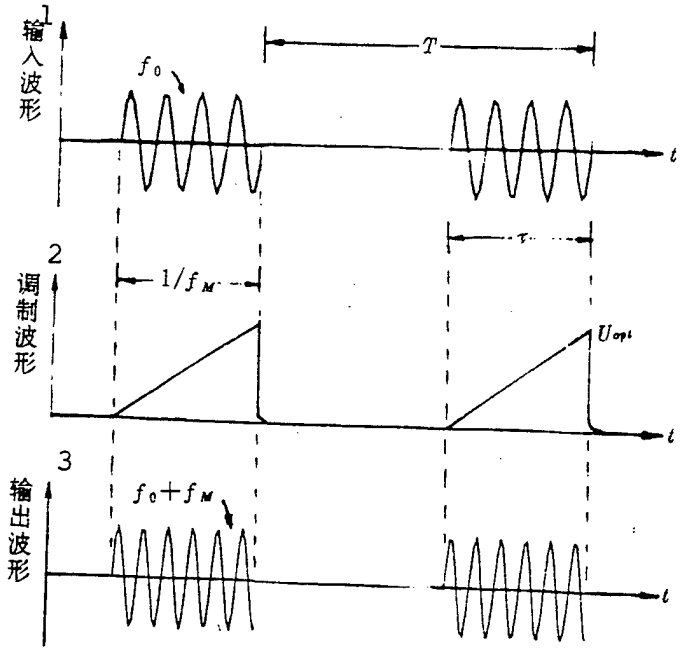

Fig. 1. Waveforms derived through modulation using single optimal sawtooth wave within pulse width
KEY: 1 - input waveform 2 - modulated waveform
3 - output waveform

The majority of pulse Doppler radars adopt a radio frequency coherence system. Generally, to ensure an extremely high stability of radio frequency, main oscillation amplification plus pulse modulation is preferred. With this arrangement, for a better analysis, we can replace the waveforms in Fig. 1 with the waveform integration method shown in Fig. 2 with regard to total coherence radars.

Following is a brief description of the waveform integration method:

$S_1(t)$ is a sine wave with frequency f_0, which turned into a sine wave $S_3(t)$ with frequency f_0+f_m after optimal modulation using a sawtooth wave $S_2(t)$ with frequency f_m. Then, by

multiplying $S_3(t)$ with $S_4(t)$, the video frequency pulse train with pulse width τ and the same repetition period and input pulse, we finally obtained $S_5(t)$, the radio frequency pulse train modulated with frequency shift, whose carrier frequency is f_0+f_{m0}.

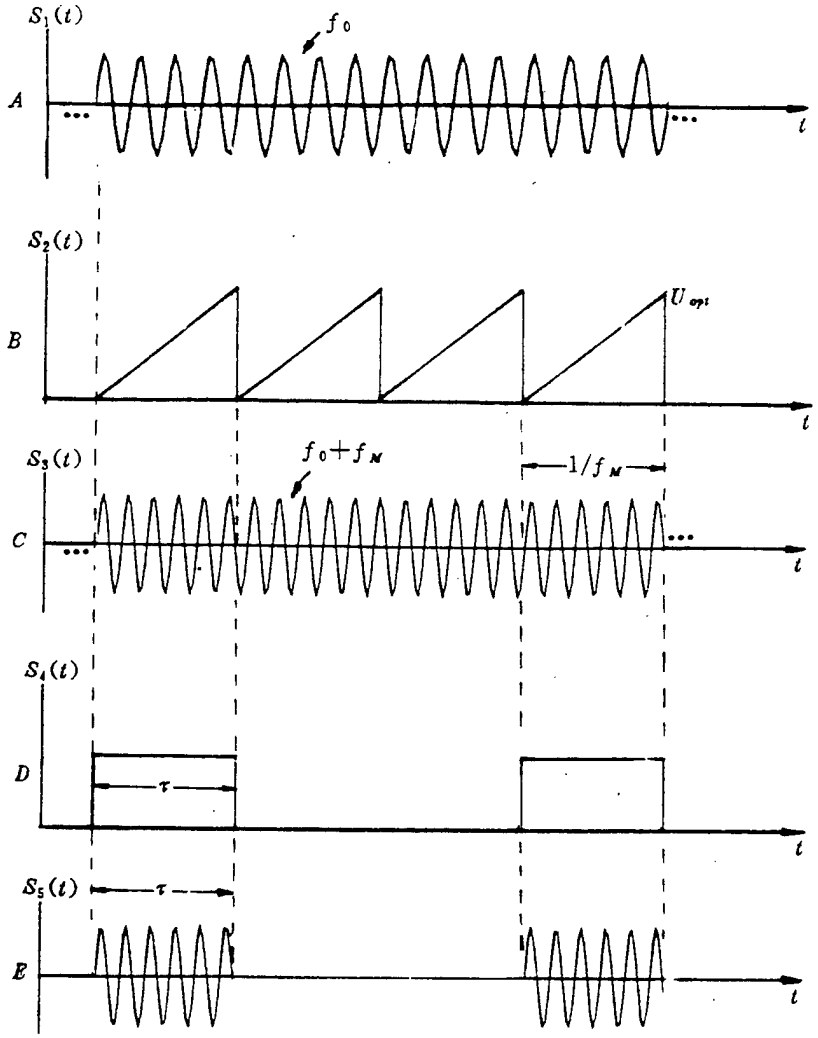

Fig. 2. Generation of waveforms in Fig. 1 using waveform integration method

Let $S_1(t)=\cos\dot{\omega}_0 t$, with an amplitude unit 1; $S_2(t)$ is a forward sawtooth wave with an amplitude U_{opt} and repetition frequency f_m; $S_3(t)=\cos(\omega_0+\omega_m)t$; $S_4(t)=\mathrm{Rep}_T[\mathrm{Rect}(t/\tau)]$.

According to the Fourier transform rules presented in reference [1], $S_3(f)$ and $S_4(f)$, the frequency spectra of $S_3(t)$ and $S_4(t)$, can be derived:

$$S_3(f) = \frac{1}{2}[\delta(f - f_0 - f_m) + \delta(f + f_0 + f_m)] \tag{1}$$

$$S_4(f) = F\tau \cdot \mathrm{comb}_F \cdot \mathrm{sinc}(f\tau) = F\tau \sum_{n=-\infty}^{\infty} \mathrm{sinc}(nF\tau) \cdot \delta(f - nF) \tag{2}$$

where n is a random integer.

Since $S_5(t) = S_3(t) \cdot S_4(t)$, then $S_5(f) = S_3(f) \otimes S_4(f)$

$$= \frac{1}{2}F\tau \sum_{n=-\infty}^{\infty} \mathrm{sinc}(nF\tau)\{\delta(f - nF) \otimes [\delta(f - f_0 - f_m) + \delta(f + f_0 + f_m)]\}$$

According to the convolution formula for two "δ" functions, the following can be obtained:

$$S_5(f) = \frac{1}{2}F\tau \sum_{n=-\infty}^{\infty} \mathrm{sinc}(nF\tau)[\delta(f - f_0 - f_m - nF) + \delta(f - nF + f_0 + f_m)] \tag{3}$$

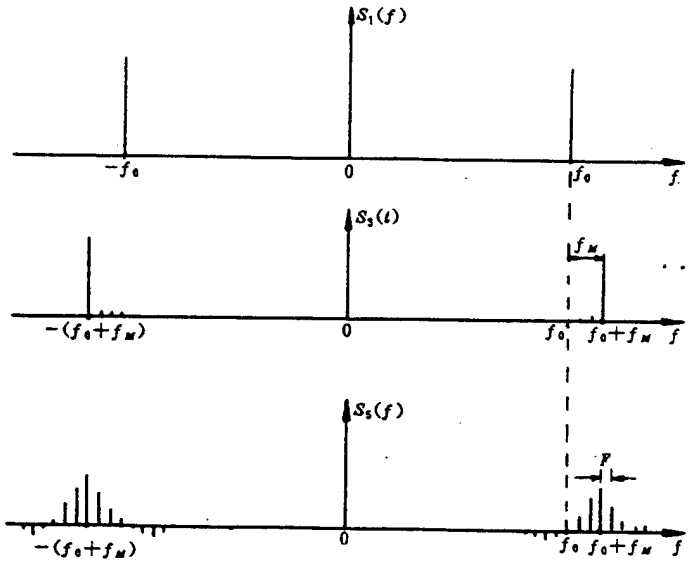

Fig. 3. Spectrograms of $S_1(f)$, $S_3(f)$ and $S_5(f)$

$S_5(f)$ is the spectrum function of the radio frequency pulse that underwent frequency shift, and its carrier frequency changed from f_0 to f_0+f_m. It is symmetrically distributed on positive and negative frequencies. The spectrum of $S_5(f)$ is plotted in Fig. 3.

For a better analysis, we assumed that the frequency shift f_m is integer times (three times in the figure) of the pulse repetition frequency F. However, this is not an indispensable condition because the relationship between f_m and F could be random, which does not affect the calculation results.

The foregoing analysis indicates that theoretically it is possible to realize the optimal modulation within a pulse width. Nevertheless, actual radar parameters show that with an excessively large frequency shift value ($\Delta\dot{\omega}$), the main spectral line cannot fall within the bandwidth of the radar Doppler filter and may result in interference energy loss, decrease or even total failure.

Reference [5] states that to avoid too many range gates, it would be desirable that the working ratio of the pulse Doppler radar d be in the range of 0.5-0.1. We designed $d_{max}=0.5$.

Pulse Doppler radars usually a adopt high pulse repetition frequency. For tactical requirements, the minimum value of the high pulse repetition frequency also should conform to the relative speed of twice the speed of sound. At the X-waveband, the Doppler frequency corresponding to twice the speed of sound velocity is approximately 40kHz. If the high repetition frequency designed can only satisfy the requirement for four times the speed of sound, then $PRF_{min}=80kHz$, so:

$$\tau_{max} = \frac{d_{max}}{PRF_{min}} = 6.25\mu s$$

The period of sawtooth wave, which corresponds to the lowest frequency shift value, is $T_m = \tau_{max} = 6.25\mu s$.

Here, the lowest modulating frequency can be derived as

$$\Delta f_{min} = \frac{1}{6.25\mu s} = 160\text{kHz}$$

while the passband of the Doppler filter set is

$$\Delta f_{d\Sigma} \leqslant \text{PRF}_{min} = 80\text{kHz} < \Delta f_{min}$$

It is obvious that the frequency shift is far overreaches the passband of the Doppler filter. In this case, although part of the energy still can enter the radar, the loss of jamming power is enormous, which will be discussed as follows.

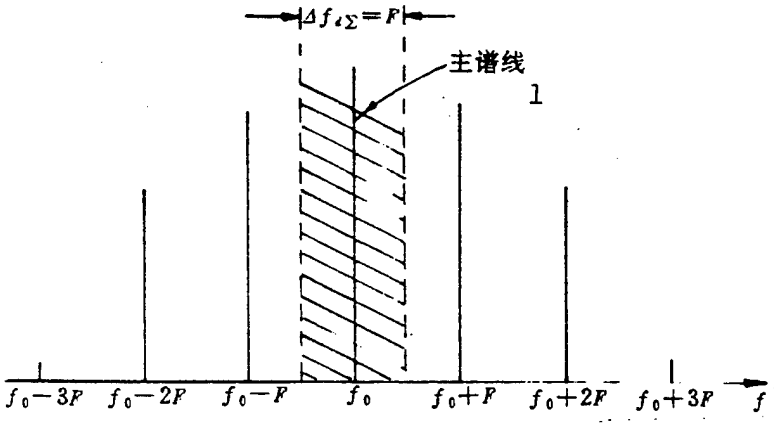

Fig. 4. Relationship between the passband of filter set of pulse Doppler radar $\Delta f_{d\Sigma}$ and repetition frequency (F)
KEY: 1 - principal spectral line

Fig. 4 shows the relationship between the passband of the Doppler filter set of the PD radar $\Delta f_{d\Sigma}$ and pulse repetition frequency F.

It is known that as the principal spectral line moves, other spectral lines will move correspondingly. Thus, if the principal spectral line moves out of the passband of the Doppler filter set $\Delta f_{d\Sigma}$, there should be another spectral line ($f_0 \pm NF$), which will fall into $\Delta f_{d\Sigma}$ and still produce a certain jamming effect.

(1) $NF=f_m$ (N is a positive integer not equal to zero): At this moment, the jamming signal generated due to modulation, coinciding with the Doppler signal of the target, does not create any jamming effect, because the modulation can only move the non-principal spectral line ($f_0 \pm NF$) in the figure to the position of the principal spectral line f_0.

(2) $NF \neq f_m$: It can be seen from Fig. 4 that when the modulated spectral line appears in front of or behind its original position, it can produce a certain deception effect. If the jamming energy is larger than the radar return wave energy, the radar can only see the jamming signal, but if the jamming energy and radar return wave energy are almost equal, the radar can see both the actual target and the deceptive jamming at the same time and become somewhat perplexed.

(3) It is desirable that the direction of the frequency shift be opposite to the direction of the Doppler frequency shift of the actual target, i.e., changing the "approaching velocity" to "departing velocity", and changing the "departing velocity" to "approaching velocity". As a result, the deceptive effect can be enhanced, and the frequency shift can be larger and thereby does not move out of the passband of the Doppler filter set.

(4) Instead of the principal spectral line, if the Nth spectral line that deviates from the principal spectral line enters the radar receiver, then, it will suffer from an energy loss since its energy is less than the energy of the principal

spectral line. The amount of loss can be calculated in accordance with the "sinc function". Generally speaking, the farther away it deviates from the principal spectral line, the larger its energy loss can be.

From the foregoing analysis on the frequency shift modulation within pulse width, the following conclusions can be drawn:

In realizing frequency shifting within a pulse width, it is extremely difficult for the principal spectral line to lie within the passband of the Doppler filter due to a large shift value. However, one of the other low-energy spectral lines will definitely enter the radar receiver and produce a certain jamming effect. The degree of this effect completely depends on the jamming energy as well as the "jamming/signal" ratio inside the receiver.

It is very difficult for the actual equipment to realize frequency shift modulation technology within pulse width, because in a multiple signals environment or to counterattack multiple threat radars, the interferometer has to deal with entirely different signals. Under such circumstances, to realize the optimal frequency shift modulation within the width of each pulse would be an extremely complex task in terms of signal discrimination and control techniques.

2. Realization of Optimal Modulation in Several Pulse Periods

2.1 Optimal Frequency Shift Modulation in the State of Radar Detection

The video frequency pulse waveforms generated in the state of radar detection are shown in Fig. 5.

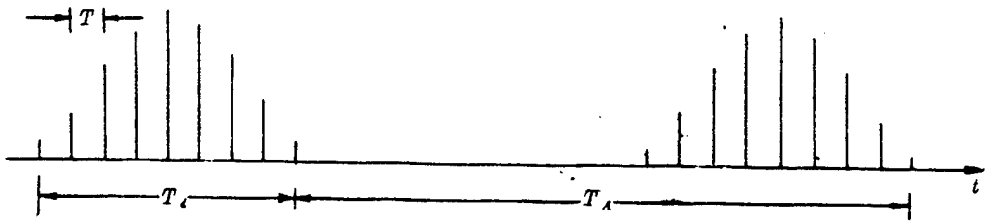

Fig. 5. Plot of pulse waveforms derived in state of radar detection

In Fig. 5, T_d is the width of the pulse set; T=1/F is pulse repetition period; τ is pulse width; T_A is antenna scan period.

Suppose the optimal sawtooth wave modulation is conducted in a set of pulses, i.e., let the period of the sawtooth wave be equal to T_d. Since this is a PD radar, we again employ the waveform integration method as shown in Fig. 6.

In Fig. 6, $S_1(t)$ is an input pulse with carrier frequency f_0, pulse width τ and period T; $S_2(t)$ is a continuous-wave signal that corresponds to $S_1(t)$; $S_3(t)$ is a sawtooth wave which is used to modulate $S_2(t)$; $S_4(t)$ is a continuous wave generated after the optimal modulation of $S_2(t)$ by $S_3(t)$, with a frequency f_0+f_m ($f_m=1/T_d=1/T_m$); $S_5(t)$ is a rectangular pulse series, whose width and period are equal to those of the input pulse; $S_6(t)$ is a square wave with a width $T_d(T_d=T_m)$; $S_7(t)$ is the product of $S_6(t)$ and $S_5(t)$, i.e., $S_5(t)$ is selected only from T_d. Finally, through multiplying $S_4(t)$ by $S_7(t)$, we obtain S(t), the modulated output radio frequency pulse with a carrier frequency f_0+f_m.

The optimal modulation of radio frequency pulse series $S_1(t)$ using optimal sawtooth wave $S_3(t)$, i.e., velocity jamming to pulse Doppler radar is equivalent to optimal modulation of original sine wave $S_2(t)$ of $S_1(t)$ using sawtooth wave $S_3(t)$, and then multiplied by rectangular pulse series of $S_7(t)$. This is

the core of the waveform integration method as discussed in this paper.

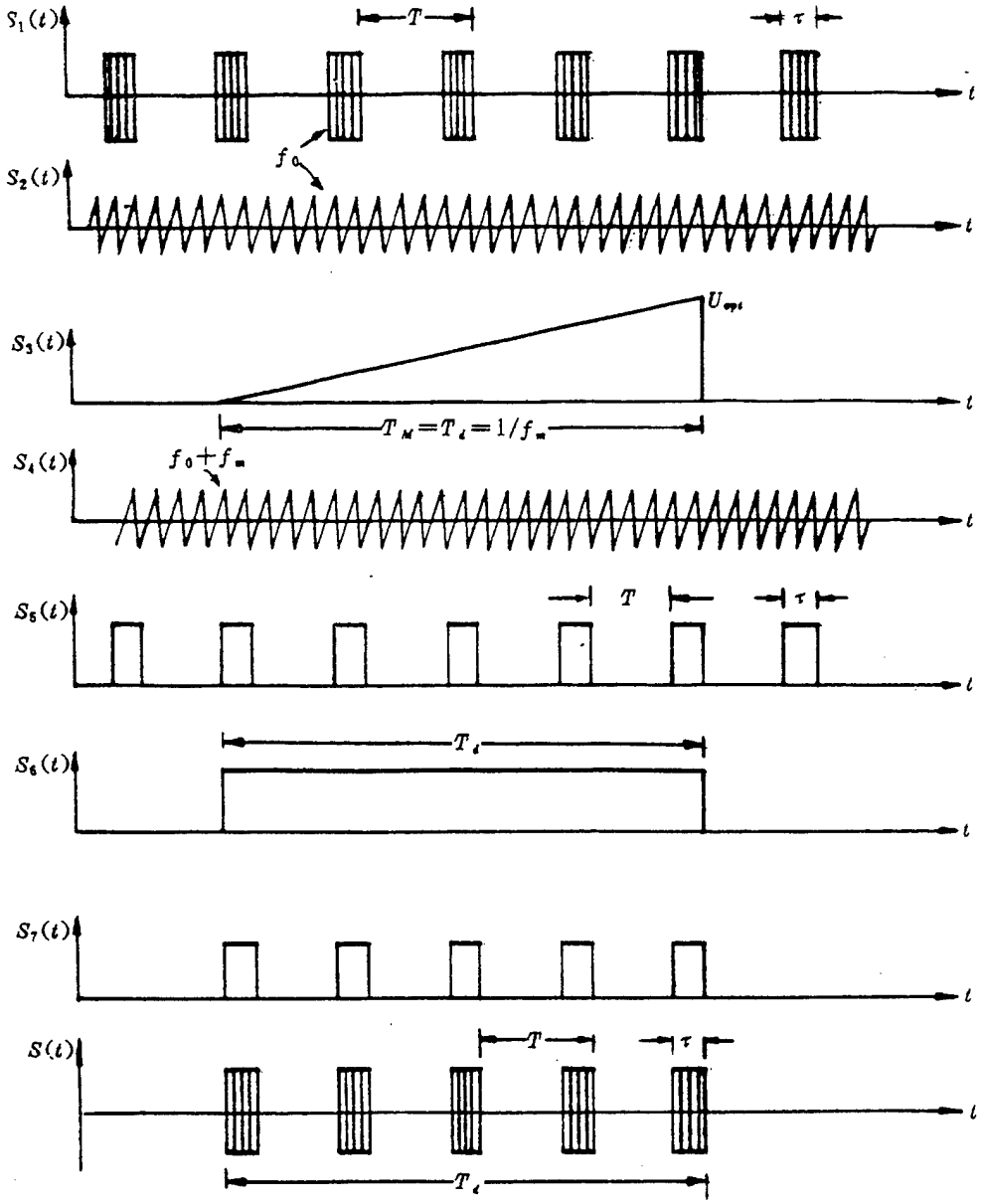

Fig. 6. Waveform integration method used to realize optimal phase modulation within width of a pulse set

Following is an analysis of the S(t) spectrum

$$S_6(t) = \mathrm{Rect}(t/T_d) \tag{4}$$

$$S_5(t) = \mathrm{Rep}_T[\mathrm{Rect}(t/T_d)] \tag{5}$$

$S_4(t)$ is the waveform derived after the optimal modulation of $S_2(t)$ by $S_3(t)$, so

$$S_4(t) = \cos(2\pi f_0 t + 2\pi f_m t) = \cos 2\pi (f_0 + f_m)t \tag{6}$$

According to the principles of the waveform integration method and Fourier analysis,

$$S(t) = S_4(t) \cdot S_5(t) \cdot S_6(t)$$

Let: $S_4(t) \longleftrightarrow S_4(f); S_5(t) \longleftrightarrow S_5(f); S_6(t) \longleftrightarrow S_6(f); S(t) \longleftrightarrow S(f)$

thus:
$$S(f) = S_4(f) \otimes S_5(f) \otimes S_6(f) \tag{7}$$

Since:
$$S_6(f) = T_d \mathrm{sinc}(T_d f) \tag{8}$$

$$\begin{aligned} S_5(f) &= F \cdot \mathrm{comb}_F \cdot [\tau \mathrm{sinc}(\tau f)] \\ &= F\tau \cdot \mathrm{comb}_F \cdot \mathrm{sinc}(f\tau) \\ &= F\tau \mathrm{sinc}(\tau f) \sum_{n=-\infty}^{\infty} \delta(f - nF) \\ &= F\tau \sum_{n=-\infty}^{\infty} \mathrm{sinc}(nF\tau)\delta(f - nF) \end{aligned} \tag{9}$$

$$S_4(f) = \frac{1}{2}[\delta(f - f_0 - f_m) + \delta(f + f_0 + f_m)] \tag{10}$$

the following can be obtained from Eqs. (8) and (9):

$$\begin{aligned} S_6(f) \otimes S_5(f) &= T_d \mathrm{sinc}(T_d f) \otimes F\tau \sum_{n=-\infty}^{\infty} \mathrm{sinc}(nF\tau)\delta(f - nF) \\ &= T_d F\tau \sum_{n=-\infty}^{\infty} \mathrm{sinc}(nF\tau)[\mathrm{sinc}(T_d f) \otimes \delta(f - nF)] \\ &= T_d F\tau \sum_{n=-\infty}^{\infty} \mathrm{sinc}(nF\tau)\mathrm{sinc}[T_d(f - nF)] \end{aligned} \tag{11}$$

Eq. (11) represents two sinc functions, and it is known from their parameters that the larger function encloses the smaller one. Their spectrograms are plotted in Fig. 7.

From Eqs. (10) and (11), the following can be derived:

$$\begin{aligned} S(f) &= S_4(f) \otimes S_5(f) \otimes S_6(f) = T_d F\tau \sum_{n=-\infty}^{\infty} \mathrm{sinc}(nF\tau)\mathrm{sinc}[T_d(f - nF)] \otimes \frac{1}{2}[\delta(f - f_0 - f_m) \\ &- \delta(f + f_0 + f_m)] = \frac{1}{2} T_d F\tau \sum_{n=-\infty}^{\infty} \mathrm{sinc}(nF\tau)\{\mathrm{sinc}[T_d(f - nF)] \otimes \delta(f - f_0 - f_m) \\ &- \mathrm{sinc}[T_d(f - nF)] \otimes \delta(f + f_0 + f_m)\} = \frac{1}{2} T_d F\tau \sum_{n=-\infty}^{\infty} \mathrm{sinc}(nF\tau)\{\mathrm{sinc}[T_d(f - f_0 - f_m - nF)] \\ &+ \mathrm{sinc}[T_d(f + f_0 + f_m - nF)]\} \end{aligned} \tag{12}$$

Similarly, Eq. (12) is also composed of two functions the way that the larger function encloses the smaller one as in Fig. 7. The difference lies in the fact that Eq. (12) is symmetrically distributed on the positive and negative frequencies, while in Fig. 7, the central frequency is zero. The spectrogram of $S(f)=S_4(f)\otimes S_5(f)\otimes$ is plotted in Fig. 8. Its amplitude occupies half the figure because its energy is evenly distributed on the positive and negative frequencies.

It can be seen from Fig. 8 that the energy of the modulated signal, i.e., the jamming energy is distributed in the smaller sinc function. The main lobe of either sinc function has a width $\Delta f_s=2/T_d$ (calculated from zero). In other words, each spectral line of the radio frequency pulse signal has turned into a stretch of continuous spectrum that blocks several Doppler filters. If the energy is sufficiently large, jamming signals will appear in all corresponding filters to form blocking jamming. The evaluation range of concrete parameters is given through examples as follows:

Suppose τ=1μs; T=10μs; T_d=10T=100μs

then:

$$\Delta f_s = \frac{2}{T_d} = \frac{2\times 10^6}{100} = 20\text{kHz}$$

Since the passband of the Doppler filter set

$$\Delta f_{d\Sigma} = F = \frac{1}{T} = 100\text{kHz}$$

thus:

$$\frac{\Delta f_s}{\Delta f_{d\Sigma}} = \frac{20}{100} = 0.2$$

i.e., due to energy spread, the single enlarged spectral line blocks 20% of the passband of the Doppler filter set.

If the bandwidth of a small Doppler filter from the Doppler filter set is evaluated in the range 100-200Hz, then the foregoing result indicates that 20% of passband blocking signifies that 100-200 small Doppler filters are blocked.

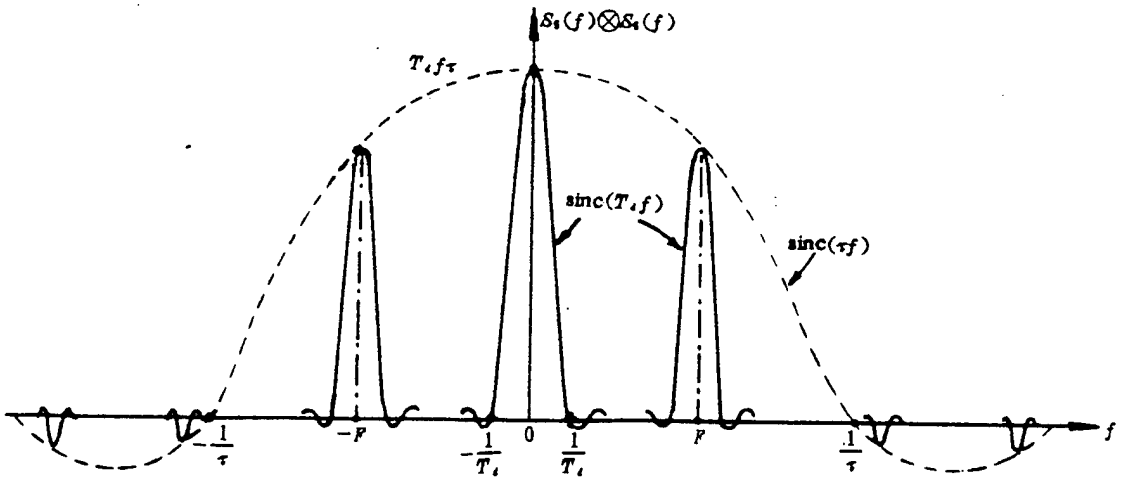

Fig. 7. Spectrogram of $S_5(f)\otimes S_4(f)$

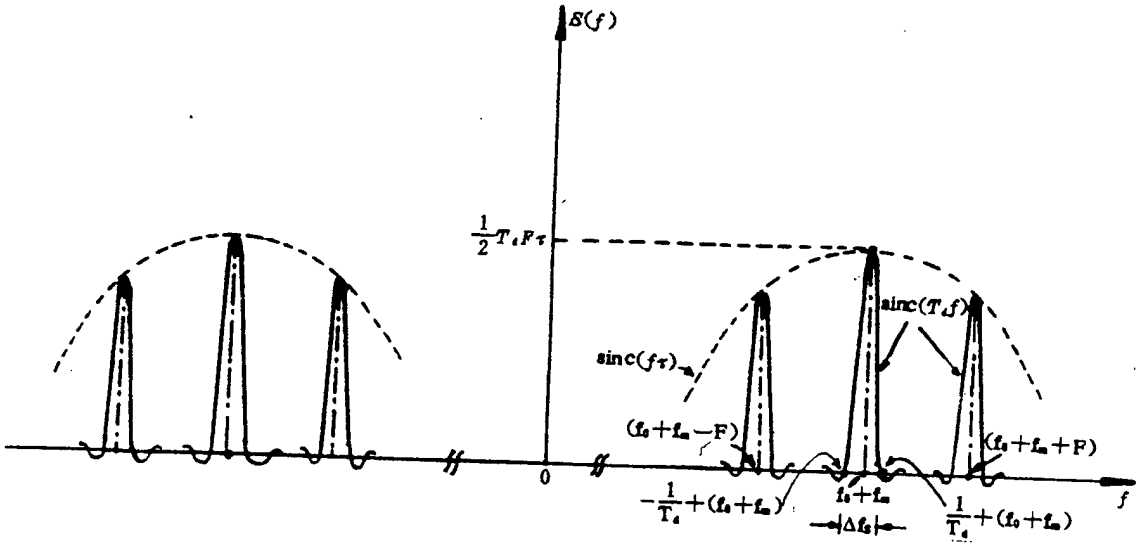

Fig. 8. Spectrogram of $S(f)=S_4(f)\otimes S_5(f)\otimes S_5(f)$

2.2. Optimal Frequency Shift Modulation During Radar Tracking

This kind of modulation is similar to optimal modulation during the state of radar detection as described above except that the radar pulse is an unlimited series, and therefore the modulating sawtooth waves are continuous one after another. Fig. 9 shows the waveforms derived in this modulation.

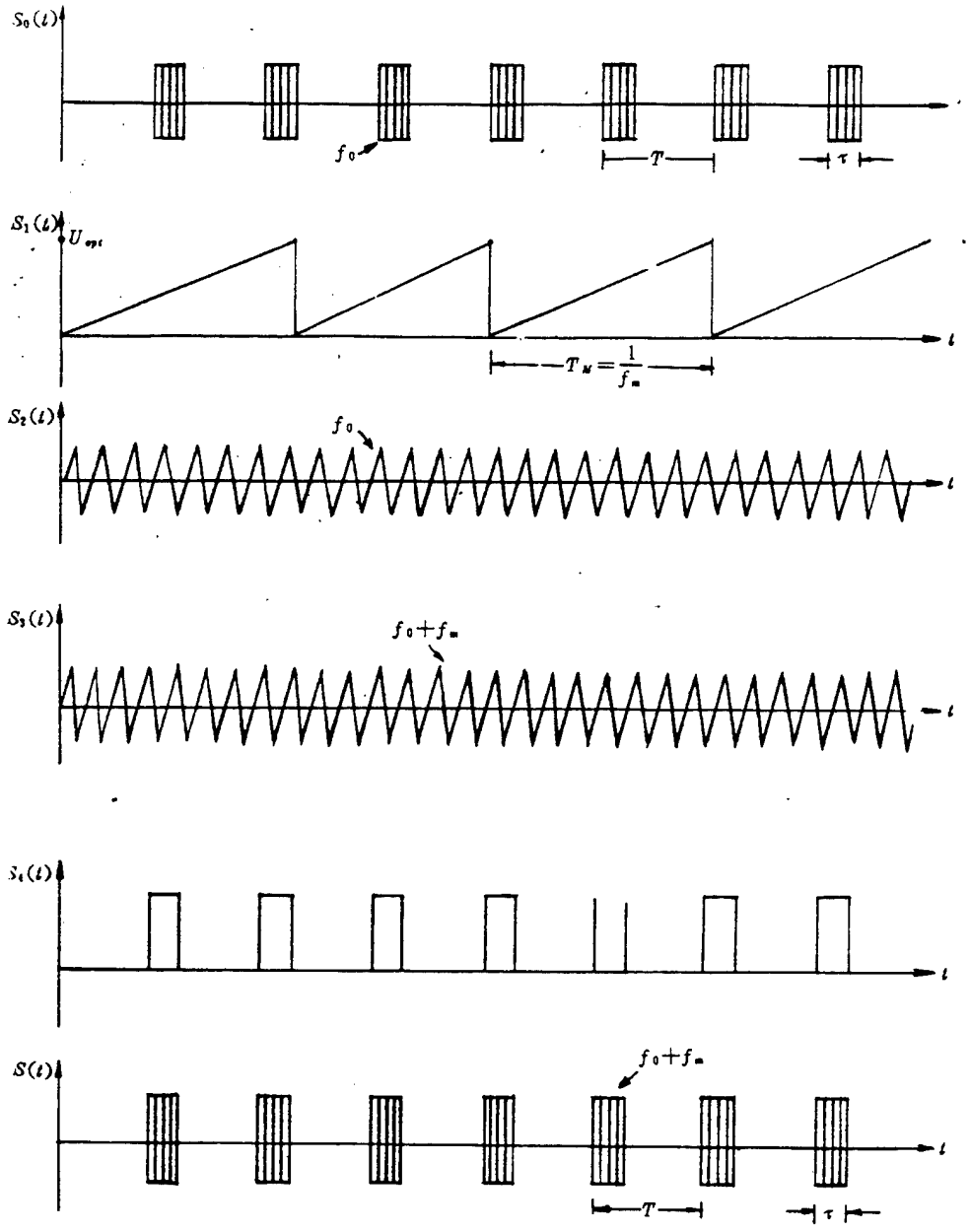

Fig. 9. Waveforms generated during modulation of unlimited pulse series by using continuous sawtooth waves

In the figure, the characteristics of individual waveforms are highlighted, while the other features are similar to those of the foregoing waveforms. Here, we used the continuous wave optimal modulation method.

Since: $$S_1(t) = \cos 2\pi f_0 t \tag{13}$$

thus: $$S_3(t) = \cos(2\pi f_0 t + 2\pi f_m t) = \cos 2\pi (f_0 + f_m) t \tag{14}$$

Here we obtain: $$S_3(f) = \frac{1}{2}[\delta(f - f_0 - f_m) + \delta(f + f_0 + f_m)] \tag{15}$$

While: $$S_4(t) = \mathrm{Rep}_T[\mathrm{Rect}(t/\tau)] \tag{16}$$

thus: $$S_4(f) = F\mathrm{comb}_F \cdot [\tau \mathrm{sinc}(\tau f)] \tag{17}$$

Since: $$S(t) = S_4(t) \cdot S_3(t) \tag{18}$$

thus: $$S(f) = S_4(f) \otimes S_3(f)$$

$$= F\mathrm{comb}_F[\tau \mathrm{sinc}(\tau f)] \otimes \frac{1}{2}[\delta(f - f_0 - f_m) + \delta(f + f_0 + f_m)]$$

$$= \frac{1}{2} F\tau \sum_{n=-\infty}^{\infty} \mathrm{sinc}(nF\tau)\delta(f - nF) \otimes [\delta(f - f_0 - f_m) + \delta(f + f_0 + f_m)]$$

$$= \frac{1}{2} F\tau \sum_{n=-\infty}^{\infty} \mathrm{sinc}(nF\tau)[\delta(f - f_0 - f_m - nF) + \delta(f + f_0 + f_m - nF)] \tag{19}$$

S(f) is two sets of δ functions symmetrical at zero. The amplitude of each set of δ functions can be divided into seven segments in accordance with the sinc($f\tau$) function. The maximum value appears on $f=\pm(f_0+f_m)$, whose spectrogram is plotted in Fig. 10.

A comparison between Figs. (8) and (10) suggests that modulating a set of pulses with a single sawtooth wave is roughly equivalent to modulating a continuous pulse series with continuous sawtooth waves. The only difference is that the former is a frequency spectral band, while the latter is a frequency spectral line. This is totally determined by whether or not the pulse train is a periodic function, without any connection to the modulation itself.

2.3. Modulation within a Limited Number of Pulses Using a Limited Number of Sawtooth Waves

Another kind of modulation, which is intermediate between the foregoing two cases, is qualitatively introduced in this section. Introducing this modulation is of practical interest because an absolute periodic function actually does not exist. It can be imagined that the spectrogram resulting from this modulation must be the spectrogram between Figs. 8 and 10, which is a narrow frequency spectral band close to a spectral line. During this modulation, the broader the pulse set, the more sawtooth waves are involved in modulation, and the closer to a spectral line the spectral band can be; or otherwise, it tends to be a wide spectral band.

2.4. Negative Sawtooth Wave Modulation

The foregoing analysis is based on the assumption that the sawtooth wave is positive. However, a negative sawtooth wave can also lead to a similar result except that the direction of frequency shift is opposite to that in the case of a positive sawtooth wave. In other words, following the optimal modulation with a negative sawtooth wave, the carrier frequency of the radio frequency pulse has decreased by $f_{\text{д}}$, or the frequency has decreased compared to that before modulation, i.e., it has imitated the negative Doppler frequency shift. Apart from this, the rest is the same as in modulation with a positive sawtooth wave. This was supported experimentally.

3. Qualitative Analysis of Non-optimal Modulation

In practical operation, the sawtooth wave cannot completely satisfy two optimal conditions: optimal amplitude and flyback time equal to zero, while the frequency shift that cannot meet these two conditions is not considered as absolutely ideal because it will carry residual carrier wave and high-second harmonic wave. The experimental result indicates that in modulating continuous waves using a sawtooth wave with excellent linearity and flyback time less than 10%, the spectrum varies

regularly with the change of the amplitude of the sawtooth wave as shown in Fig. 11.

The experiment with continuous waves shows that a single sideband modulator that proves to be satisfactory in engineering can well realize modulation. This technology has long been used in equipment with desirable results. Even though absolutely ideal conditions can hardly be met, this technology can satisfy technological requirements in engineering as long as its frequency energy is hopefully 10-20dB larger than that of other frequencies. This conclusion drawn from the experiment with continuous waves is also applicable to pulse Doppler radars, because such radars extract only one spectral line from the pulse spectrum, and a single spectral line just represents a continuous sine wave signal.

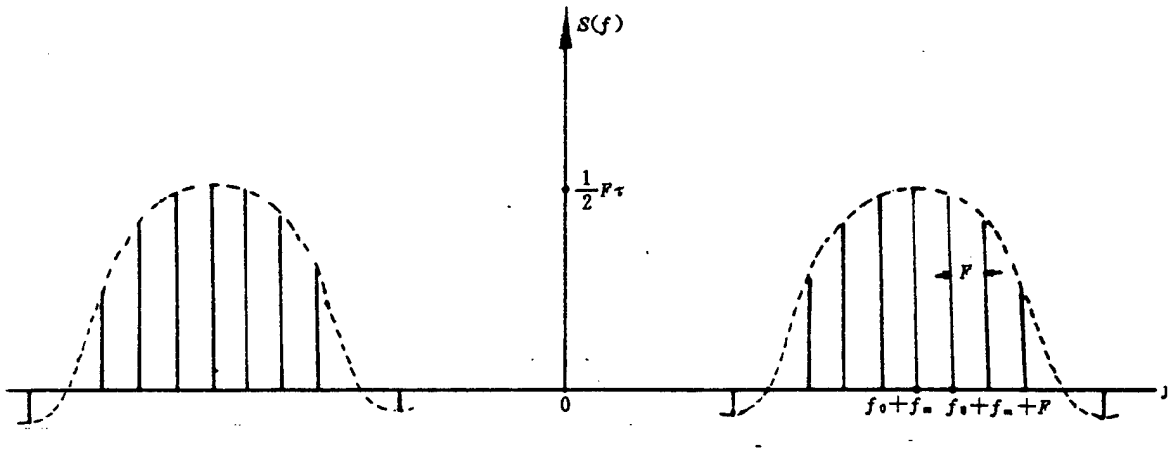

Fig. 10. Spectrum generated through modulation of an unlimited pulse train using continuous sawtooth waves

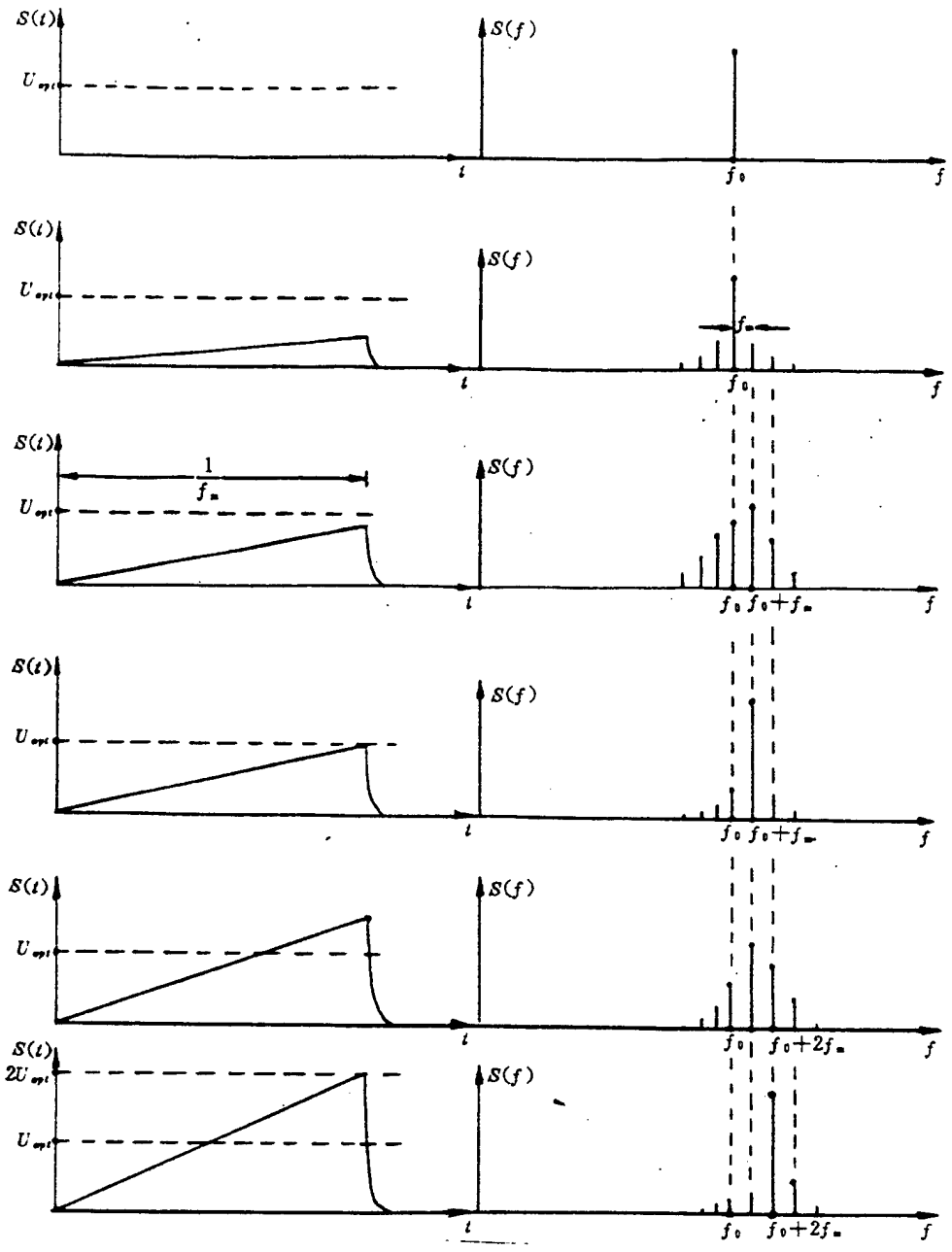

Fig. 11. Variation of modulated spectrum with amplitude of sawtooth waves

4. Conclusions

It is feasible to realize velocity jamming of the commonly used radio frequency coherent pulse Doppler radars with the jamming technology based on sawtooth wave modulation, which is

designed to deal with CW radars. Sawtooth waves can be used for modulation at any time and continuously, or once in several pulse periods. As a result of modulation, the radio frequency received by the radar will move one modulating frequency value upward or downward so as to achieve deception effects. It is also possible that multitarget jamming appears in the Doppler filter set. During optimal modulation, sweep frequency sawtooth waves can be used to create velocity pull (VGPO).

Modern radars are normally equipped with auxiliary techniques for velocity discrimination, such as range differentiation. Therefore, velocity jamming alone may not produce ideal effects. For optimal jamming effects, it would be advisable to employ a combination of several jamming patterns, such as synchronous realization of distance deception and velocity deception.

REFERENCES

1 Burdic W S. Radar Signal Analysis. Prentice Hall Inc. 1968

2 瓦金 C A. 无线电干扰与无线电技术侦察基础. 北京:科学出版社,1977

3 布赖姆 E O. 林群译. 快速付里叶变换. 上海:上海科技出版社,1979

4 The Serrodyne Frequency Translator. Proc. IRE, February, 1957

5 动目标指示雷达、连续波雷达和脉多雷达在杂波性能方面的比较. IRE International Convention Record, Vol. 9, Part 5, 1961

Appendix: Fourier Transform and Convolution Characteristics

(1) If $S(t)=\cos 2\pi f_c t$, the corresponding spectrum is:

$$S(f)=\frac{1}{2}[\delta(f-f_0)+\delta(f+f_0)]$$

(2) If time function is Rect(t), its spectrum is $S(f)=\text{sinc}(f)$.

(3) If time function is $\text{Rep}_T \cdot S(t)$, its spectrum is $S(f)=|F|\,\text{comb}_F \cdot g(f)$, in which: $S(t) \leftrightarrow g(f)$; $F=1/T$.

(4) If $S_1(t)=\delta(t-t_0)$; $S_2(t)=\delta(t-t_1)$, then: $S_1(t) \cdot S_2(t)=\delta(t-t_0-t_1)$.

(5) If $S(t)=\text{Rect}(t/T_d)$, its frequency spectrum is $S(t)=|T_d|\,\text{sinc}(T_d f)$.

(6) If $S_1(t)$ is multiplied by $S_2(t)$, its spectrum is $S(t)=S_1(f) \otimes S_2(f)$, in which: $S_1(t) \leftrightarrow S_1(f)$; $S_2(t) \leftrightarrow S_2(f)$.

(7) The formula for the comb coefficient of the frequency domain is: $\text{comb}_F=\sum_{n=-\infty}^{\infty}\delta(f-nF)$

(8) If $S_1(f)$ is convolved with $\delta S_1(f) \otimes \delta(f-nF)=S_1(f-nF)$, then

$$S_1(f) \otimes \delta(f-nF)=S_1(f-nF)$$

Notes: (1) Rep_T is the repetition factor with a period T.

(2) $\leftrightarrow$ is the symbol for the Fourier transform pair.

(3) comb_F is the comb function with F as the repetition frequency.

(4) Rect(t) is the symbol for rectangular function of time t.

(5) $\otimes$ is the symbol for convolution integration.

This paper was received on January 10, 1996.

NOISE MODULATION TECHNIQUE BASED ON AMPLITUDE MODULATION METHOD

He Min

Research Institute No. 26
Ministry of Electronic Industry
Chengdu

ABSTRACT: A new noise modulation technique based on an amplitude modulation method is proposed in this paper, following an analysis of the conventional noise technique based on the phase modulation method. This method, low in cost, convenient in use and reliable in performance, features several advantages including better suppression of carrier frequency, stable modulating noise width, and lower requirements for noise sources. A comparative test on PD radars shows that the noise modulation technique based on the amplitude modulation method is feasible and efficient in realizing jamming, and proves to be superior to the conventional noise modulation technique based on phase modulation method.

KEY WORDS: phase modulation, amplitude modulation, noise modulation, noise jamming.

0. Introduction

Noise has been regarded as an efficient radar-jamming means. For noise to become a realistic threat to radars, it is necessary to insert the noise into the passband of radars in every possible way. For this purpose, noise should be modulated at or close to the radar carrier frequency so that it can be carried by the carrier frequency into the radar passband and undermine normal radar operation. To ultimately disable radar operation, the width of the modulating noise should be broader than the passband

of the radar receiver, i.e.,

$$\Delta N > \Delta R \tag{1}$$

where ΔN is the noise spectrum width after modulation; ΔR is the passband of the radar receiver.

The conventional method of modulating noise onto the carrier frequency is to apply noise in modulating phases. It has been used as an exclusive method to achieve this goal thus far. In earlier times, the noise modulation of phases was realized directly on traveling wave tubes taking advantage of their phase shift properties. While in recent years, with the appearance of high-speed electronically modulating phase shifters, noise modulation of phases has been conducted on electronically modulating phase shifters in many engineering designs. Whatever the device, the mechanism of noise modulation is based on "phase modulation".

In practical applications, the author found that the above-mentioned method, though conventional, has some disadvantages while applied. First, this method does not have adequate capabilities to suppress carrier waves, which is actually a fatal defect in terms of electronic countermeasures, because if the carrier wave has not been suppressed, not only can it not produce any jamming effect, but it also becomes a radar return wave intensifier and therefore may expose itself too soon. Secondly, this method has stringent requirements on noise amplitude.

In response to this situation, a new noise modulation method is proposed in this paper, which is essentially based on "amplitude modulation". The conventional amplitude modulation method as one of the noise modulation methods has been rejected due to some inherent problems and shortcomings. However, with the development of modern device technology, it is possible now

to solve and overcome these problems and shortcomings.

The modulation method presented in this paper can not only effectively overcome those inherent amplitude modulation shortcomings, but achieve much better results compared with phase modulation as well. Moreover, the equipment needed for this method is much cheaper than a phase modulator, and the requirement for the amplitude of noise has reduced by one order of magnitude.

1. Theoretical Analysis

1.1. Phase Modulation

The phase modulation oscillation can be expressed with the following formula:

$$U = U_m \cos[\omega_0 t + aS(t) + \varphi_0] \tag{2}$$

To simplify the analysis, let S(t) be simple sine oscillation with frequency Ω_1 and initial phase Φ_1 . Eq. (2) can be written as:

$$U = U_m \cos[\omega_0 t + m_1 \cos(\Omega_1 t + \Phi_1) - \varphi_0] \tag{3}$$

To accurately expand the phase modulation oscillation with a random modulation index m_1 to the sum of simple functions, we use the following formula:

$$e^{im_1 \sin x_1} = \sum_{n=-\infty}^{+\infty} J_n(m_1) e^{inx_1} \tag{4}$$

where $J_n(m_1)$ is n-order Bessel function of m_1. Let $\Omega_1 t + \Phi_1 = x$, then Eq. (3) can be rewritten as

$$\begin{aligned} U &= U_m \cos(\omega_0 t + m_1 \sin x_1 + \varphi_0) \\ &= U_m \mathrm{R_e}[e^{i(\omega_0 t + \varphi_0)} e^{im_1 \sin x_1}] \\ &= U_m \sum_{n=-\infty}^{+\infty} J_n(m_1) \cos(\omega_0 t + nx_1 + \varphi_0) \end{aligned} \tag{5}$$

By substituting $x_1 = \Omega_1 t + \Phi_1$ in Eq. (5), we obtain

$$U = U_m \sum_{n=-\infty}^{+\infty} J_n(m_1) \cos[(\omega_0 + n\Omega_1)t + n\Phi_1 + \varphi_0] \tag{6}$$

and the modulation index

$$m_1 = \frac{\varphi_{max} - \varphi_{min}}{2} \tag{7}$$

From Eq. (6) and Bessel function properties, some simple conclusions concerning phase modulation oscillation can be derived as follows:

a. When a signal with frequency Ω_1 is employed for modulation, the phase modulation oscillation can be expressed with the sum of oscillation with carrier wave frequency ω_0 and the amounts of side frequency oscillation which are symmetrically distributed on both sides of the carrier frequency and have a frequency $\omega_0 \pm n\Omega_1$. The frequency difference between them is Ω_1 .

b. The amplitude of each component is $U_m J_n(m_1)$.

c. Theoretically, the amount of side frequency is unlimited, yet starting from $n=m_1+1$, the amplitude of side frequency rapidly decreases with increase in n. Thus, in reality, it can be assumed that the amount of side frequency is equal to $2(m_1+1)$.

It is known from the above discussion that the spectrum width of the phase modulation oscillation and the amplitude of the spectral line are closely associated with the modulation index m_1. Fig. 1 shows the spectrum distribution with different modulation index m_1.

Let us discuss the side frequency during single sine oscillation with frequency Ω_1 as an example. Suppose the modulator is a 360^0 electronically modulating phase shifter, and the phase modulation is a limiting value $0\text{-}360^0$, then according to the definition of modulation index, we obtain

$$m_1 = \frac{\varphi_{max} - \varphi_{min}}{2} = \frac{360^\circ \sim 0^\circ}{2} = 180^\circ = \pi$$

From this we can derive the amount of side frequency at this moment as:

$$n = 2(m_1 + 1) = 2(\pi + 1) \approx 8 .$$

1.2 Amplitude Modulation

The oscillation in amplitude-based noise modulation can be expressed with the following formula:

$$\begin{aligned} U &= U_m(t)\cos(\omega_0 t - \varphi_0) \\ &= U_c[1 + N(t)]\cos(\omega_0 t + \varphi_0) \end{aligned} \tag{8}$$

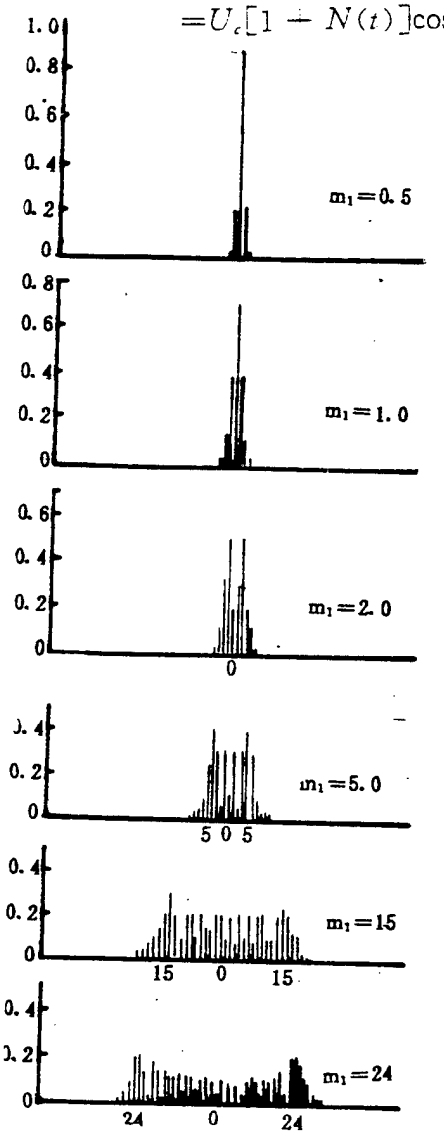

Fig. 1. Spectrogram of phase modulation oscillation with different m

The noise function N(t) can be described as the sum of the amounts of sine oscillation. Thus, Eq.(8) can be written as:

$$U=U_c[1+\sum_{k=1} M_k\cos(\Omega_k t+\Phi_k)]\cos(\omega_0 t+\varphi_0) \tag{9}$$

where Ω_k is the angular frequency of modulating noise; M_k is the partial modulation index. To simplify the subsequent discussion, we assume N(t) is simple sine oscillation with angular frequency Ω_1, then we obtain

$$U=U_c[1+M_1\cos(\Omega_1 t+\Phi_1)]\cos(\omega_0 t+\varphi_0) \tag{10}$$

Making use of triangle function relations, we rewrite Eq. (10) as

$$U=U_c\{\cos(\omega_0 t+\varphi_0) + \frac{M_1}{2}\cos[(\omega_0+\Omega_1)t+\varphi_0+\Phi_1] + \frac{M_1}{2}\cos[(\omega_0-\Omega_1)t+\varphi_0-\Phi_1]\} \tag{11}$$

In this way, the simplest amplitude modulation oscillation can be expressed with the sum of three sine oscillation. All the three sine oscillation feature constant amplitude, frequency and phase shift. The angular frequency of the three oscillation, respectively, is $(\omega_0-\Omega_1)$, ω_0 and $(\omega_0+\Omega_1)$, with the difference Ω_1 among them; the corresponding amplitude, respectively, is $(M_1U_c)/2$, U_c, and $(M_1U_c)/2$. Their spectral lines are shown in Fig. 2.

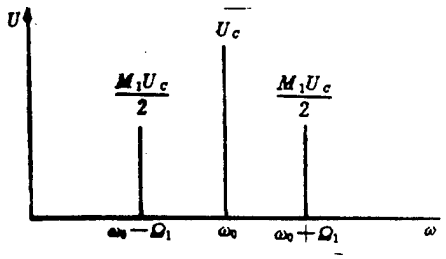

Fig. 2. Spectrum of amplitude modulation oscillation

It is known from the above analysis that an inherent shortcoming of the amplitude modulation oscillation is that it carries an extremely large carrier wave component U_c. This is

the reason why the amplitude modulation method is not accepted in general noise modulation. It is quite obvious that to apply amplitude modulation method in realizing noise modulation, our task is to decrease the carrier wave component.

1.3. Comparison between Phase Modulation and Amplitude modulation

TABLE 1. Comparison of Phase Modulation/Amplitude Modulation Characteristic Features

	调相 1	调幅 2
旁频数量*3	$2(m_1+1)$	2
频谱宽度*4	$2(m_1+1)\Omega_1$	$2\Omega_1$
剩余载频 5	$U_c J_0(m_1)$	U_c
旁频幅度 6	$U_c J_1(m_1)$	$\frac{M_1 U_c}{2}$
调制指数 7	$m_1=\frac{\varphi_{max}-\varphi_{min}}{2} \begin{matrix}\geqslant \\ < \end{matrix} 1$	$M_1=\frac{\Delta U_c}{U_c} \leqslant 1$

KEY: 1 - phase modulation 2 - amplitude modulation 3 - amount of side frequency* 4 - spectrum width* 5 - residual carrier frequency 6 - amplitude of side frequency 7 - modulation index
* Higher-second harmonic wave of modulating signal is ignored.

Table 1 shows a comparison between the characteristic features of simple single sine phase modulation and amplitude modulation. From this table, several conclusions concerning "phase-based" and "amplitude-based" noise modulation can be drawn as follows:

(1) Phase modulation normally has higher capabilities of suppressing carrier waves than amplitude modulation. Furthermore, the carrier wave-suppressing capability during phase modulation is related to modulation index m_1 in the following tendency: the larger the m_1, the better the suppression can be, while in amplitude modulation, the carrier-suppressing ability is unrelated to m_1.

(2) Amplitude of side frequency: In phase modulation, the amplitude of side frequency varies regularly with the variation of m_1 obeying Bessel function $J_n(m_1)$; while in amplitude modulation, the amplitude of side frequency varies in linear direct proportion to m_1.

(3) Spectrum width: Since m_1 could be much larger than 1 during phase modulation, its spectrum would be much broader than that in amplitude modulation and furthermore, under the precondition that the higher-second harmonic wave of the modulating signal is ignored, the amount of side frequency is much larger in phase modulation than in amplitude modulation.

It can then be concluded that compared with amplitude modulation, the phase modulation features higher capabilities of suppressing carrier waves, more abundant side frequency spectrums, i.e., it can derive broader noise spectrum width.

2. Noise Modulation

2.1. Shortcomings of Conventional Noise Modulation Method

The above analysis clearly indicates that phase noise modulation is by no means perfect. In the author's view, it suffers from at least the following shortcomings:

(1) It is not an ideal method in suppressing carrier waves, and the carrier-suppressing degree is directly related to the modulation index m. In this case, to achieve an ideal carrier-suppressing ratio, a sufficiently large modulation index m is required. To meet this condition, vigorous requirements should be posed on the electronically modulating phase shifter as well as the modulating noise level, i.e., the electronically modulating phase shifter should achieve the maximum phase shift 360^0, for which, the amplitude of the modulating noise should be

approximately 20V.

(2) With the development of electronic countermeasures, the "frequency-aiming" precision of the interferometer is growing higher and higher. To effectively utilize jamming resources, the noise modulation spectrum should be limited to a narrower width. In other words, the width of noise modulation should be limited. In this case, applying the noise modulation technology would be disadvantageous in controlling the spectrum width of noise modulation. This can be seen from Table 1, where the final modulating spectrum width is related to an uncertain factor--the modulation index m. Due to the effect of factor m, the phase modulation technology is advantageous when noise modulation spectrum is required as broad as possible. However, when the noise modulation spectrum width is required to be limited and especially, when a narrower noise spectrum is required, this technology will not be helpful.

(3) Vigorous requirements for modulating noise: A typical modern electronically modulating phase shifter generally needs a modulating voltage larger than 20V to achieve a 360^0 phase shift. Designing a noise source with such an amplitude seems to be a heavy pressure on a circuit engineer.

(4) High insertion loss: Commercial phase shifters available on the market are usually manufactured with multiple cascade connection so as to reach a 360^0 phase shift, which will inevitably lead to a fairly high insertion loss, generally more than 10dB.

(5) High cost: Whether traveling-wave tubes or electronically modulating phase shifters used for phase modulation, both devices are very expensive, particularly the electronically modulating phase shifter, which ranks first in the price list of microwave devices.

As far as amplitude modulation is concerned, the most critical problem is the excessively large residual carrier. As long as we can manage to suppress the carrier frequency, the amplitude modulation method will be feasible for noise modulation.

The carrier-suppressing technology was a problem long-since solved in telecommunication engineering. To effectively make use of transmitter power resources, the carrier frequency that does not contain any information should be suppressed during transmission with only side frequency spectrums retained. This kind of modulation is called carrier-suppressing modulator. The device used in this modulation is a balanced modulator as shown in Fig. 3, with the variation of modulated spectrums shown in Fig. 4.

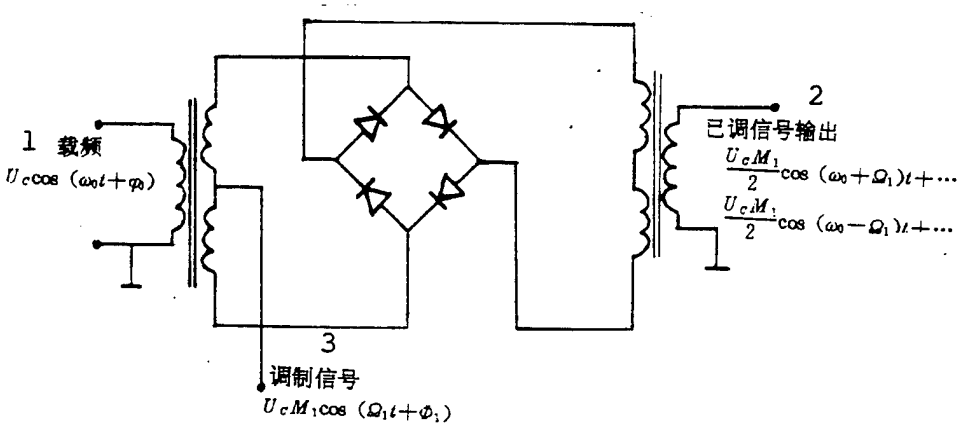

Fig. 3. Diagram showing the principle of carrier-suppressing modulator
KEY: 1 - carrier frequency 2 - modulated signal output 3 - modulating signal

Under ideal conditions, i.e., under total "balance", this modulator is capable of completely suppressing the carrier frequency at its output end. In practice, however, total balance is impossible due to the difference of circuits and devices, and a certain amount of residual carrier frequency will always be

output at the output end. Normally, carrier suppression can reach over 20dB.

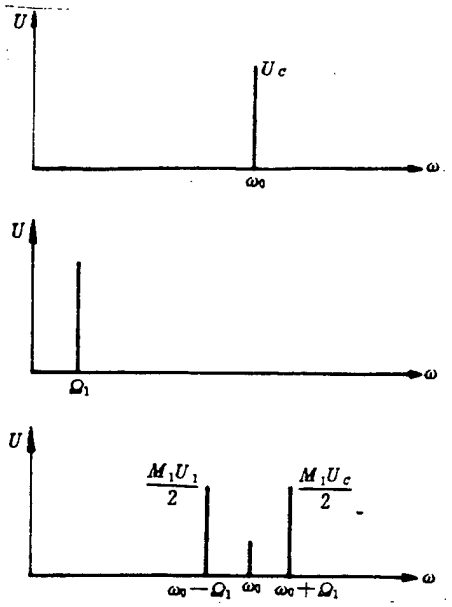

Fig. 4. Amplitude modulated spectra

2.2. Characteristics of Noise Sources

To effectively realize noise modulation, it is necessary to discuss some of the characteristics of noise sources so that we can work out appropriate requirements.

2.2.1. Noise Energy and Energy Spectra

When we talk about the output level of noise sources, we use noise power to specify it, for example, a certain noise source with an output power 100mW, etc. Sometimes we describe it directly with voltage, such as noise voltage 10V. These statements are not exactly strict, because in specifying the

characteristics of noise sources, our first concern is: on which frequency and within how broad a band the noise is, and the output power should be the "total power" within this bandwidth. Based on this point, we introduce the following formula:

$$P_n = \int_0^\infty S(\omega)\mathrm{d}\omega \tag{12}$$

where $S(\omega)$ is the density of the noise power spectrum, which is defined as noise power within the unit frequency width (W).

P_n is the sum of noise power in the whole frequency domain, i.e., the noise power that we usually measure using a power meter.

In practical applications, it is the density of noise power spectrum, not the total noise power that is interesting, because in reality, a noise power may be an extremely high value measured with a power meter, yet it appears extremely small in the expected band. Therefore, our major concern is always concentrated on the noise power in a certain band, i.e.

$$P_{n\Delta\omega} = \int_{\omega_0-\Delta\omega/2}^{\omega_0+\Delta\omega/2} S(\omega)\mathrm{d}\omega \tag{13}$$

2.2.2. Low-frequency Noise and Its Generation

It is known from spectrum analysis that to moderate a noise with bandwidth ω_0 near a carrier signal with a frequency $\Delta\omega$, the frequency range of the noise to be modulated is required to be DC~$\Delta\omega/2$. Similarly, to counterattack radars with different characteristics, the required $\Delta\omega$ is also different. For instance:

To counterattack ordinary pulse radars: DC~5MHz

To counterattack pulse Doppler radars: DC~50kHz

To effectively utilize jamming resources, we always hope

that the noise spectrum will be limited to a certain range. However, as we know, the spectrum range of any primary noise source is very broad, while in our expected low-frequency band, the density of power spectrum is extremely low. To acquire a satisfactory low-frequency noise, it is possible to move the primary noise frequency and convert it to a low-frequency noise starting from DC. The process of such moving is shown in Fig. 5.

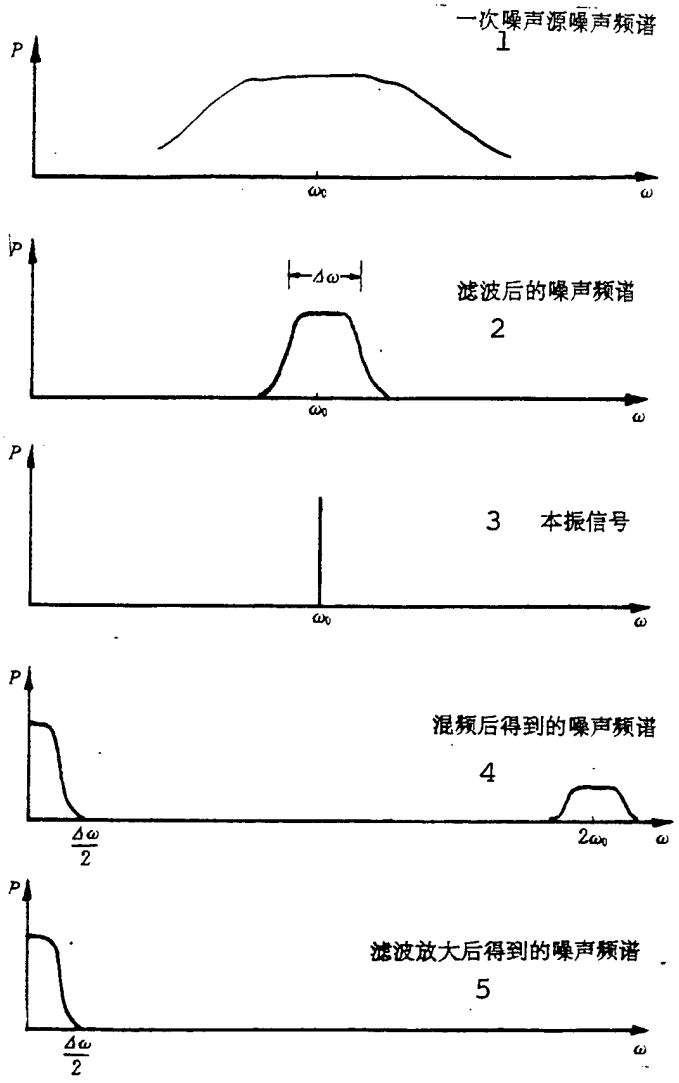

Fig. 5. Process of realizing low-frequency noise
KEY: 1 - noise spectrum of primary noise source 2 - filtered noise spectrum 3 - local oscillated signal 4 - noise spectrum after frequency mixing 5 - amplified noise spectrum through filtering

Fig. 6 is a block diagram of a circuit designed to complete the above process.

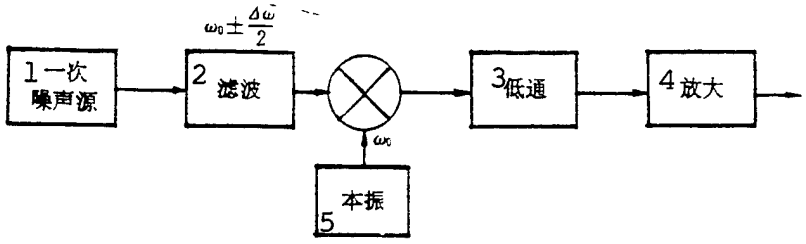

Fig. 6. Block diagram showing realization of low-frequency noise
KEY: 1 - primary noise source 2 - filtering
3 - low pass 4 - amplification
5 - local oscillation

3. Amplitude-based Noise Modulation Technology

3.1. Single Modulator-based Noise Modulation Method

The advantages of this method include simple structure, i.e., noise modulation can be realized with only one balanced modulator, and low insertion loss. A disadvantage of this method lies in the fact that it needs a fairly high level of the modulating noise to suppress carrier waves as required. Fig. 7 shows a circuit designed to realize noise modulation using this method and its spectrum variation.

3.2. Double Modulator-based Noise Modulation Method

The principle of the double modulator-based noise modulation method is: The first modulator modulates the carrier frequency and the sine oscillation with a fixed frequency, and acquires the suppressed carrier frequency as well as the generated side

frequency; then, these signals again are modulated by the second modulator, through which ideal modulation results can be derived. Fig. 8 shows how the spectrogram of this modulation is generated.

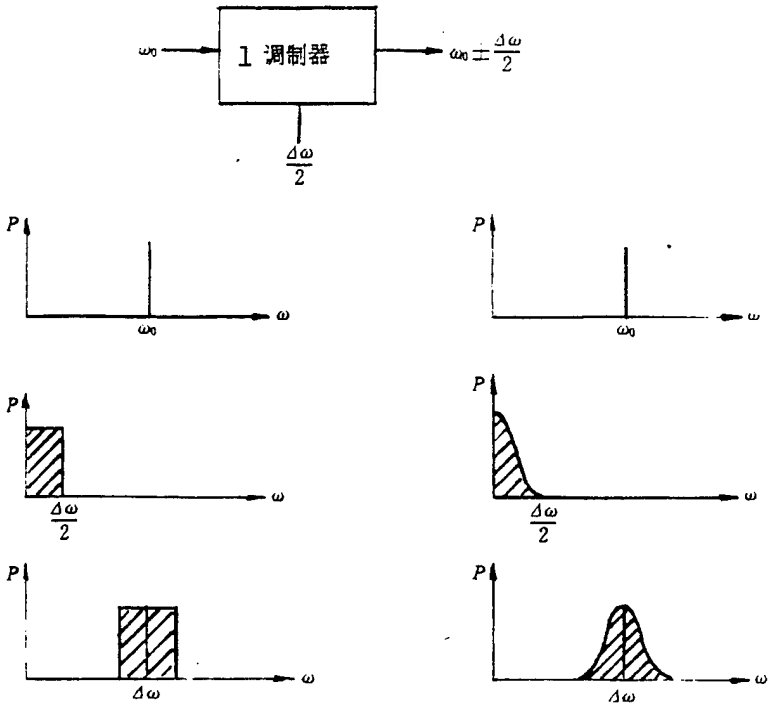

Fig. 7. Single modulator-based modulation spectrogram
KEY: 1 - modulator

With high carrier-suppressing capabilities, the double modulators are always considered as the first choice among devices, for which fairly high requirements are posed.

3.3. Parameter Selection of Modulating Signals

Suppose the width of the final noise spectrum is $\Delta\dot{\omega}$, then the related parameters should be selected in accordance with the following principles:

Frequency of sine oscillation with fixed frequency

$$\Omega = \frac{\Delta\omega}{4}$$

Spectrum width and range of noise modulation

Width: $\Delta N = \frac{\Delta\omega}{4}$

Range: $\mathrm{DC} \sim \Delta N$

Level of sine oscillation with fixed frequency

Power level should be higher than 7dBm (5mW)

Noise power

Theoretically, the noise power is required as large as possible; its minimum value should be larger than 20dBm, i.e.,

$$\int_0^{\Delta\omega} S(\omega)\mathrm{d}\omega \geqslant 20\mathrm{dBm}$$

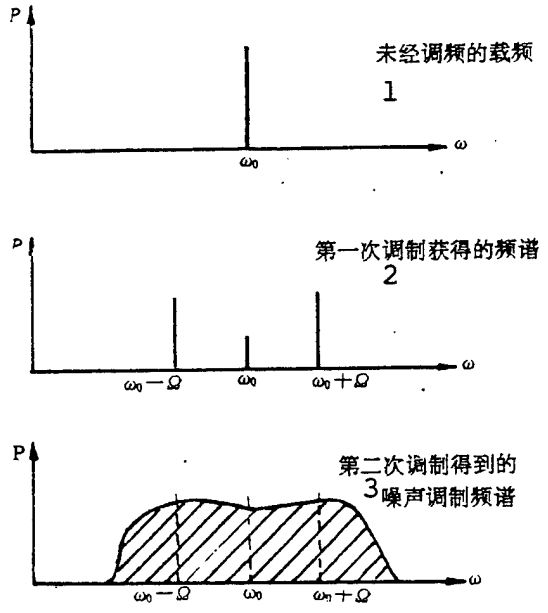

Fig. 8. Double modulator-based noise modulation spectrogram

KEY: 1 - unmodulated carrier frequency
2 - spectrum derived after first modulation 3 - noise modulation spectrum obtained after second modulation

Requirements for fixed sine and noise waveform:

Fixed sine should be sine oscillation, symmetrically distributed relative to "zero"

Noise waveform should be normal distribution noise, symmetrically distributed relative to "zero".

3.4. Comparison among Several Modulation Methods

The major indicators of several modulation methods are compared in Table 2.

TABLE 2. Comparison of Performance Among Several Modulation Methods

比 较 内 容 1	单 调 制 器 2	双 调 制 器 3	调 相 4
完成功能 5	噪声 移频 6	噪声 移频 7	噪声 移频 8
载频抑制 9	一般 10	很好 11	较差 12
插入损耗(dB) 13	<10	<20	20 左右 14
要求调制噪声频谱宽度15	$\Delta\omega/2$	$\Delta\omega/4$	$\Delta\omega$
移频信号 16	可变正弦(f) 17	可变正弦(f) 18	• 可变锯齿(f) 19
调制信号幅度(V) 20	<10	<10	>20
可靠性 21	高 22	高 23	一般 24
调制器价格 (人民币:元) 25	约 1000 26	约 2000 27	几万 28
体积、重量 29	小 30	小 31	大(进口移相器) 32 小(自研器件)

KEY: 1 - content of comparison 2 - single modulator 3 - double modulators 4 - phase modulation 5 - functions 6 - noise, frequency shift 7 - noise, frequency shift 8 - noise, frequency shift 9 - carrier suppressing 10 - average 11 - excellent 12 - poor 13 - insertion loss 14 - approximately 20 15 - required spectrum width of modulating noise 16 - frequency shift signal 17 - variable sine 18 - variable sine 19 - variable sawtooth 20 - amplitude of modulating signal 21 - reliability 22 - high 23 - high 24 - average 25 - price of modulator (RMB: Yuan) 26 - approximately 1000 27 - approximately 2000 28 - tens of thousands 29 - volume, weight 30 - small 31 - small 32 - large (imported phase shifters), small (domestically developed devices)

4. Experiments and Conclusions

With the double modulator circuit amplitude-based noise modulation technology, we experimented with pulse Doppler (PD) radars and obtained satisfactory noise jamming results. The Doppler noise modulation jamming signal with bandwidth 20kHz, generated with this technology, can totally suppress radar carrier frequency as shown in Figs. 9-11. Similarly, with the single modulator circuit noise modulation technology, we also successfully realized the goal of frequency shift in the laboratory and arrived at over 10dB carrier suppression as shown in Fig. 12.

As confirmed in both experiments and applications, the amplitude modulation-based noise modulation technology turns out to be feasible and efficient, and can therefore serve as another applicable resource in electronic warfare technology.

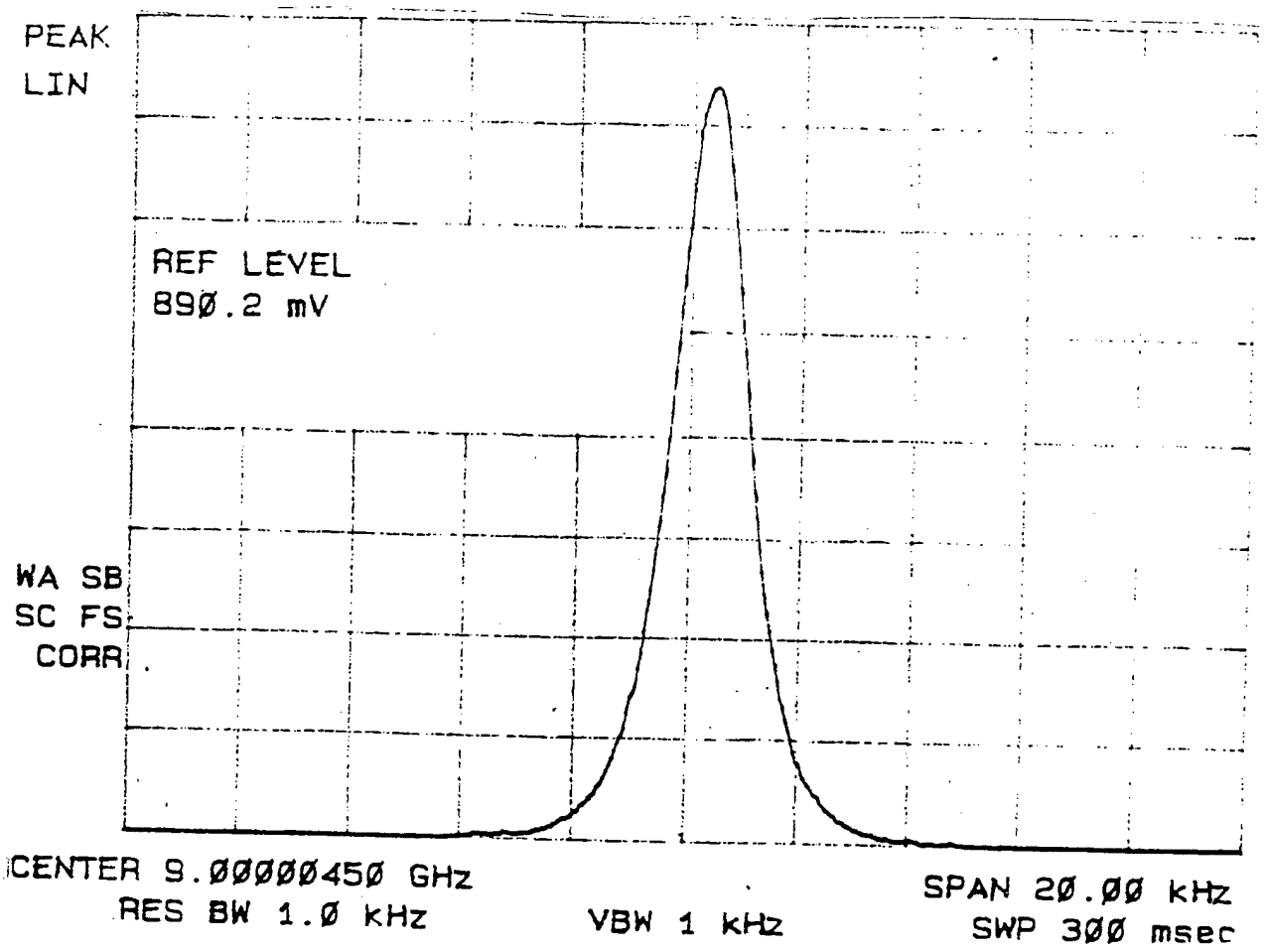

Fig. 9. Carrier frequency without noise modulation

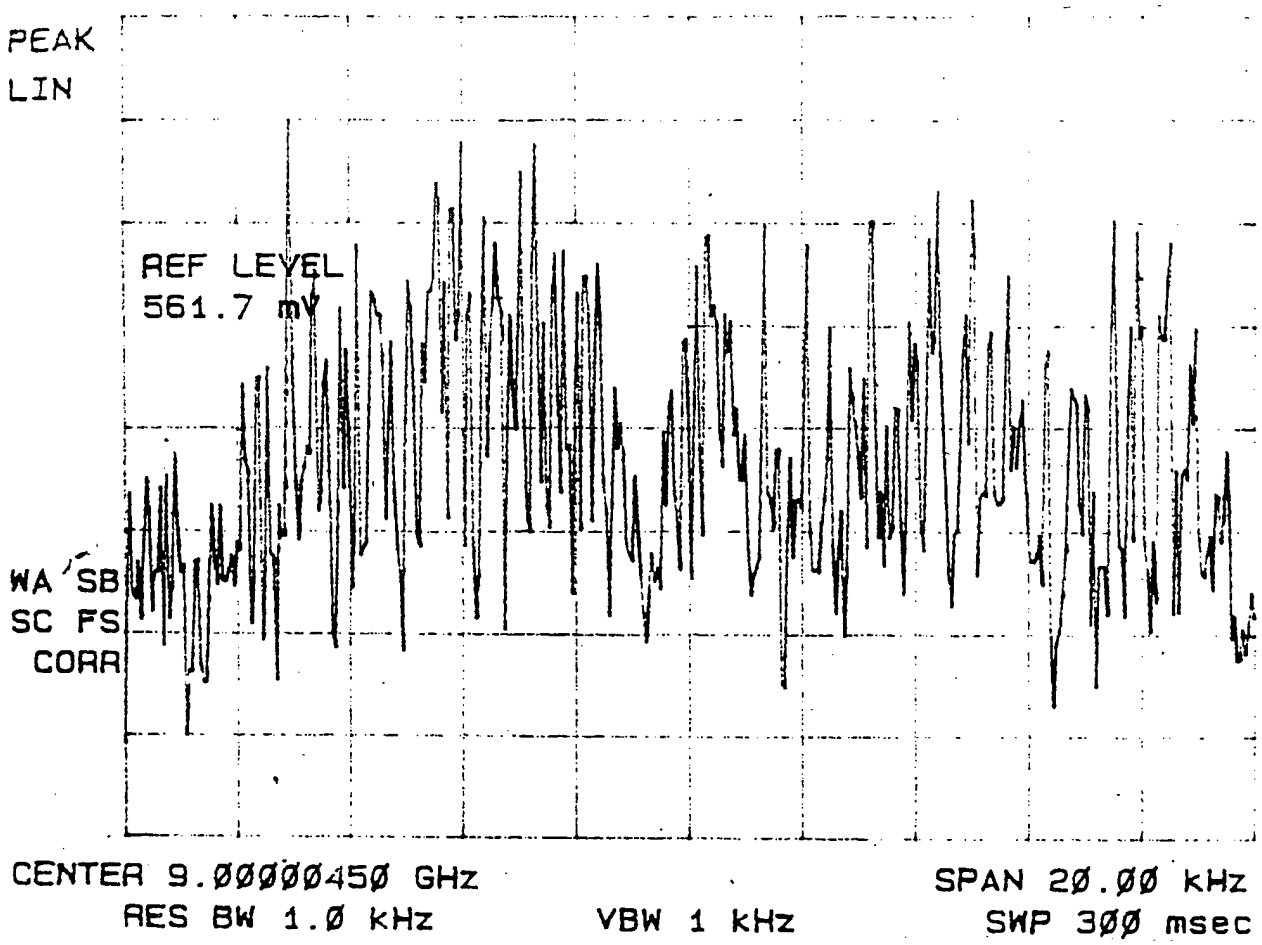

Fig. 10. Spectrum derived through Doppler low-frequency noise modulation

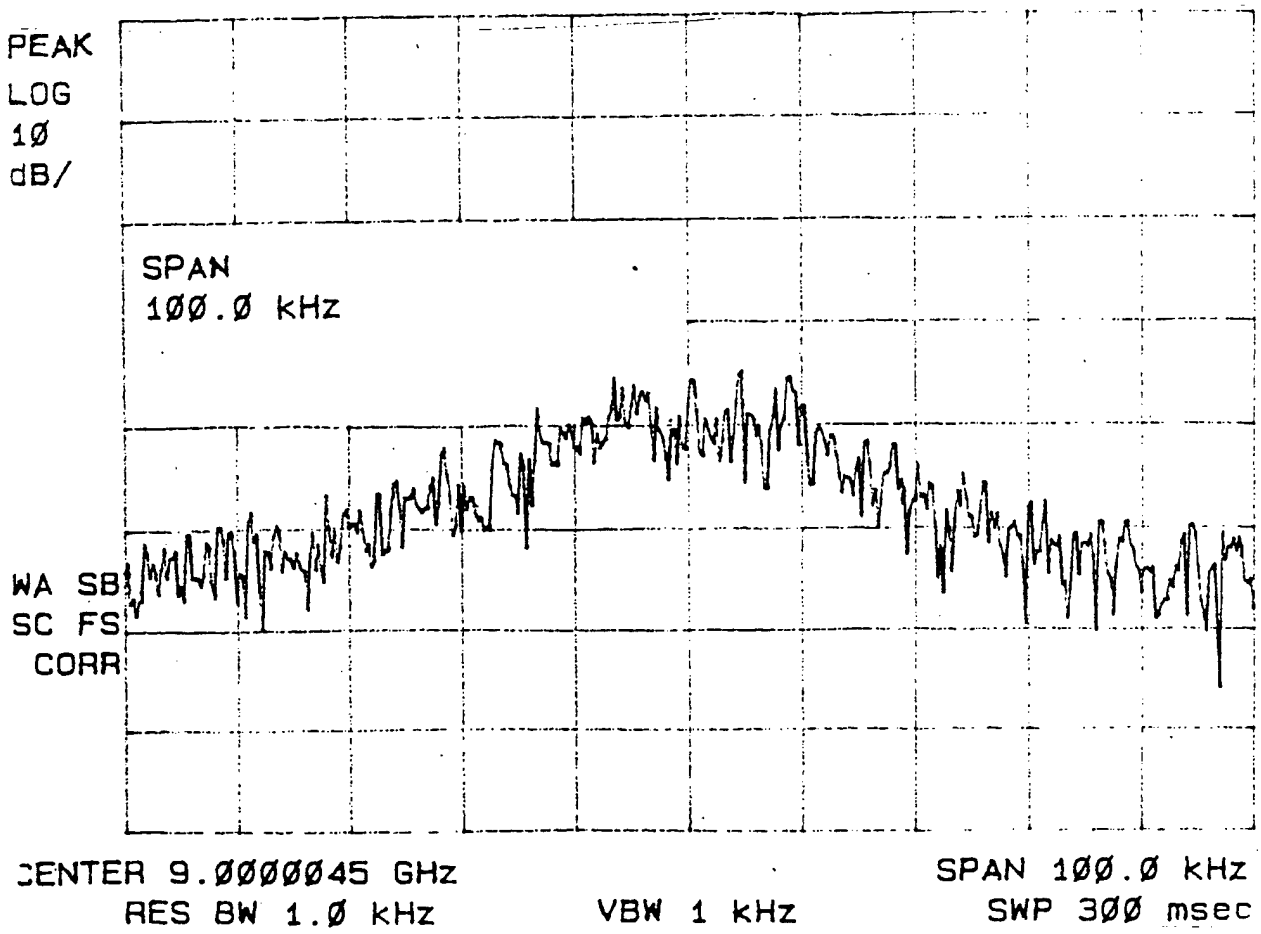

Fig. 11. Noise modulation results displayed with logarithmic coordinates

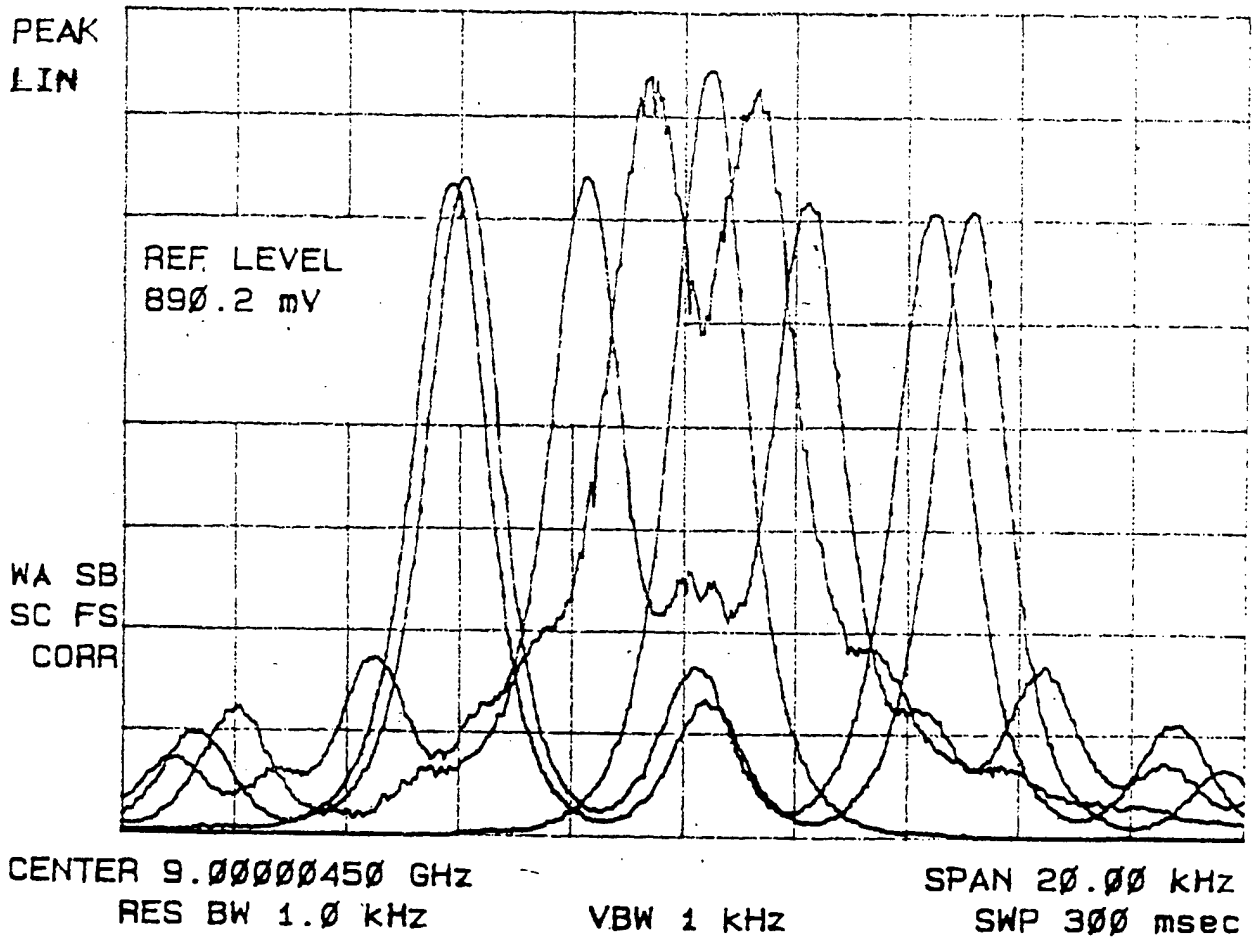

Fig. 12. Spectra formed at different instants due to frequency shift

This paper was received on January 10, 1996.